Dear Editor,

We appreciate the prompt reviews and would like to thank the two reviewers for insightful comments and suggestions on our manuscript entitled "Characteristics of fine particle matters at the top of Shanghai Tower" (MS No.: egusphere-2022-782). We have carefully considered all comments and suggestions. Listed below are our point-by-point responses to all comments and suggestions of this reviewer (Reviewer's points in black, our responses in blue).

Anonymous Referee #1

The author conducted chemical composition measurement at high altitude, expanding our understanding on aerosol chemistry at mid-upper PBL. I suggest major revision for the manuscript prior to be finally published in ACP.

Response:

We sincerely thank the reviewer for the valuable comments. These comments have been carefully addressed during revision. Please find our point-to-point response below and highlighted changes in the revised manuscript.

1. The collection efficiency was chosen as 0.5. In fact, the composition dependent CE was more precise. The author should compare these two methods and evaluate whether default CE influence NR-PM_1 species quantification.

Response:

Thanks for your suggestions. Following the composition-dependent

algorithm brought up by Middlebrook et al. (2012), we evaluated the effect of both aerosol acidity and ammonium nitrate fraction on CE, and further NR-PM_1 species quantification.

For acidic aerosols, the CE was calculated as:

$$CE_{dry} = \max\left(0.45, 1.0 - 0.73 \times \left(\frac{NH_4}{NH_{4,pred}}\right)\right), \quad [1]$$

where the $NH_{4,pred}$ was the predicted concentration of ammonium needed to neutralize the inorganic anion mass concentrations observed by the ACSM:

$$NH_{4,pred} = 18 \times \left(\frac{SO_4}{96} \times 2 + \frac{NO_3}{62} + \frac{Chl}{35.45}\right). \quad [2]$$

NH_4, SO_4, NO_3, Chl were the measured aerosol ammonium, sulfate, nitrate, and chloride mass concentrations (in μg m^{-3}), respectively. The average ratio of measured NH_4 versus predicted NH_4 was 0.78, suggesting a weak acidity. The averaged CE in each season (Table AR1) was close to 0.5. However, the year-averaged masses calculated from the acidity dependent CE were 5.7%, 4.9%, 6.3%, 5.3% and 4.8% larger than those from default CE for NO_3, SO_4, NH_4, Chl and organics.

For high ammonium nitrate fraction aerosols, the CE was calculated as:

$$CE_{dry} = \max(0.45, 0.0833 + 0.9167 \times ANMF), \quad [3]$$

where the ANMF was the ammonium nitrate mass fraction:

$$ANMF = \frac{80/62 \times NO_3}{(NH_4 + SO_4 + NO_3 + Chl + Org)}. \quad [4]$$

The Org was the measured organic mass concentrations (in μg m^{-3}). The average ANMF was 0.29, which is quite low than the threshold value (0.4) that affects CE (Middlebrook et al., 2012). The ratios of year-averaged masses calculated from the ammonium nitrate mass fraction dependent CE versus those from default CE were 0.96, 1.04, 1.00, 1.01 and 1.03 for NO_3,

SO_4, NH_4, Chl and organics, respectively.

Overall, the biases between NR-PM_1 mass concentrations calculated from composition dependent and default CE were acceptable. Thus, we revised the manuscript based on the results presented here.

Table AR1: The aerosol acidity and ammonium nitrate fraction effects on CE. The $M_{CE,acd}$, $M_{CE,anf}$, and $M_{CE,default}$ stand for the average NR-PM_1 mass calculated from the acidity dependent CE, the ammonium nitrate mass fraction dependent CE, and default CE.

	Acidity effect			Ammonium nitrate fraction effect		
	CE	$NH_4/NH_{4,pred}$	$M_{CE,acd}/M_{CE,default}$	CE	ANMF	$M_{CE,anf}/M_{CE,default}$
Spring	0.49	0.79	1.05	0.49	0.31	1.00
Summer	0.50	0.75	1.04	0.46	0.22	1.08
Autumn	0.48	0.83	1.08	0.47	0.26	1.06
Winter	0.49	0.77	1.05	0.51	0.38	0.93
All	0.49	0.78	1.05	0.48	0.29	1.01

2. PMF source apportionment was performed for entire study, with two-factor solution being resolved. Considering that the emissions sources could be different in different seasons, PMF should be done separately during each season. Did the author try to do ME-2 analysis with constrained POA profiles to improve results?

Response:

Thank you so much for the suggestion. First, we conducted unconstrained PMF source apportionments separately for four seasons. The POA factors were mixed with OOA feature (prominent m/z 44 signal) in 2-factor solutions for all four seasons (Figure AR1-4). Increasing the factor number did not help.

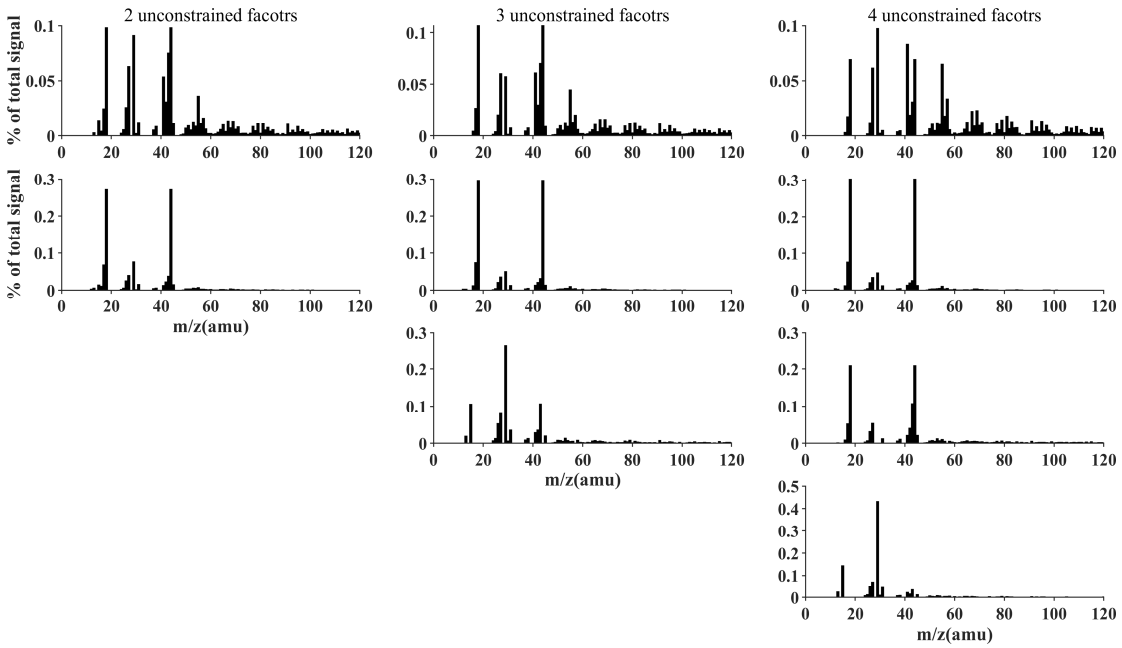

Figure AR1: Mass spectra of 2-4 factor solution from unconstrained PMF for spring.

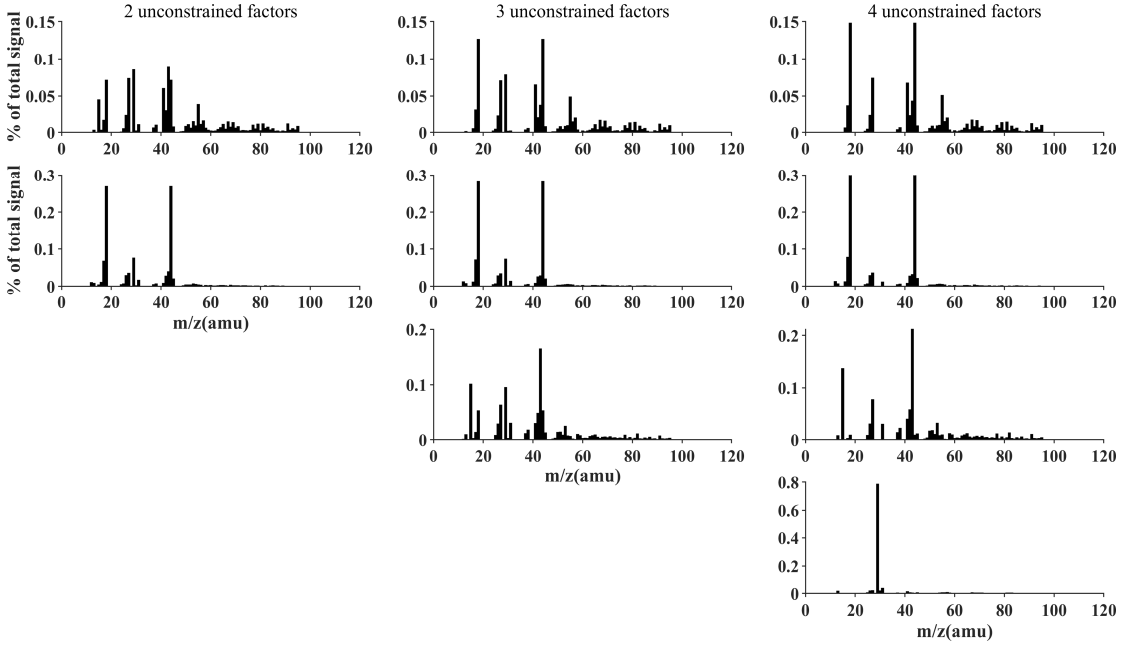

Figure AR2: Mass spectra of 2-4 factor solution from unconstrained PMF for summer.

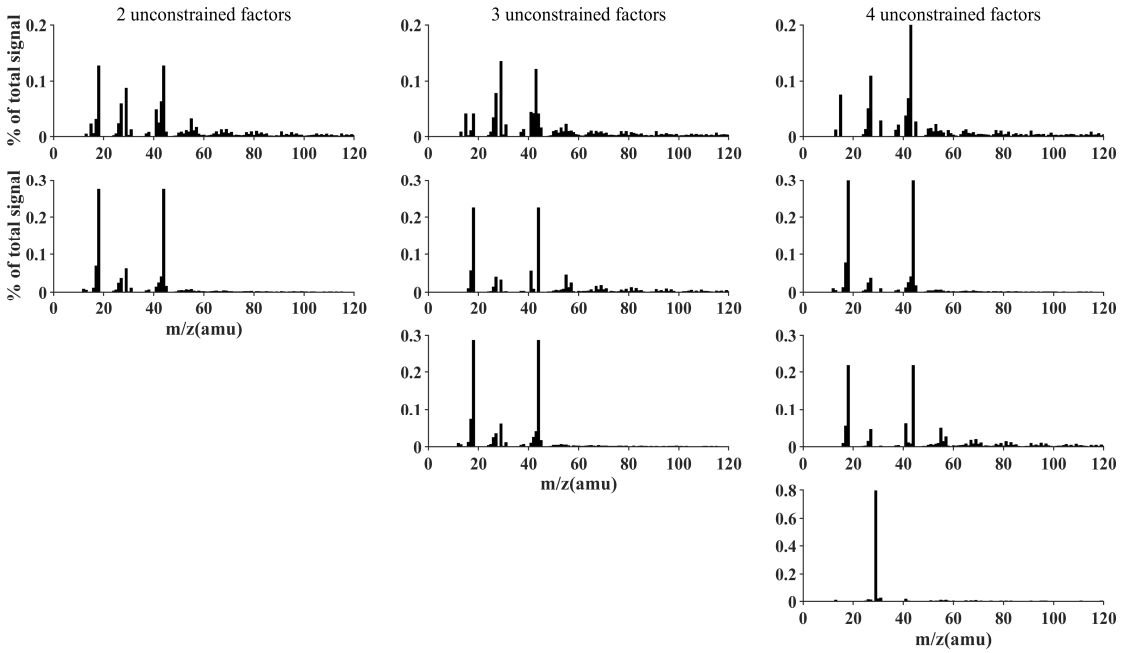

Figure AR3: Mass spectra of 2-4 factor solution from unconstrained PMF for autumn.

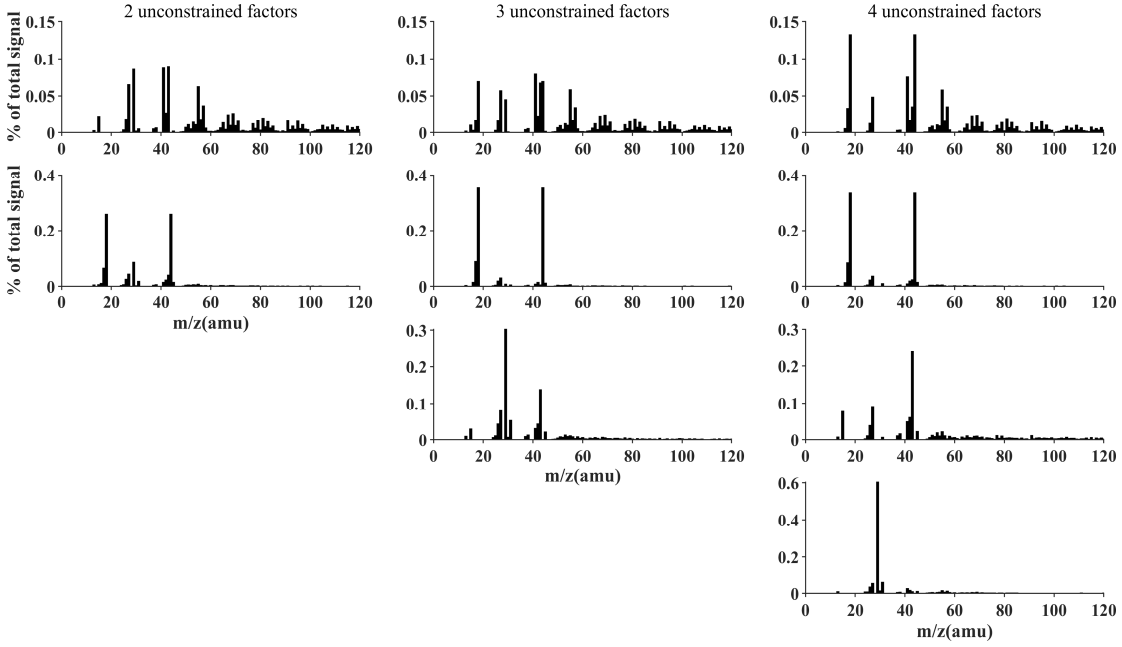

Figure AR4: Mass spectra of 2-4 factor solution from unconstrained PMF for winter.

Then, we did ME-2 analysis with a priori POA profile from the unconstrained two-factor solution for both four seasons and the entire research period. In ME-2 analysis, a coefficient called a-value was used to

constrain the spectra variation extent of the given priori factor mass spectra (Canonaco et al., 2013). First, the ME-2 analysis (a=0.1) was performed with possible factor number of 3-5 (Figure AR5-8). Besides the POA factor, all the 3-factor solutions split two OOA factors. For most cases, the two OOA factors could be identified as a MO-OOA (more oxidized OOA) and a LO-OOA (less oxidized OOA). Normally, the LO-OOA spectrum is characterized with a relatively higher peak at m/z 43 and a lower O/C ratio or f_{44} than MO-OOA. However, in winter situation, the two OOA factors had no compatible $f_{44/43}$ and f_{44}. For example, one OOA factor had higher $f_{44/43}$ but lower f_{44}, suggesting failure in clean spiting of OOA factors. As shown in Figure AR5-8, the 4 or 5 factors solutions failed splitting more meaningful factors.

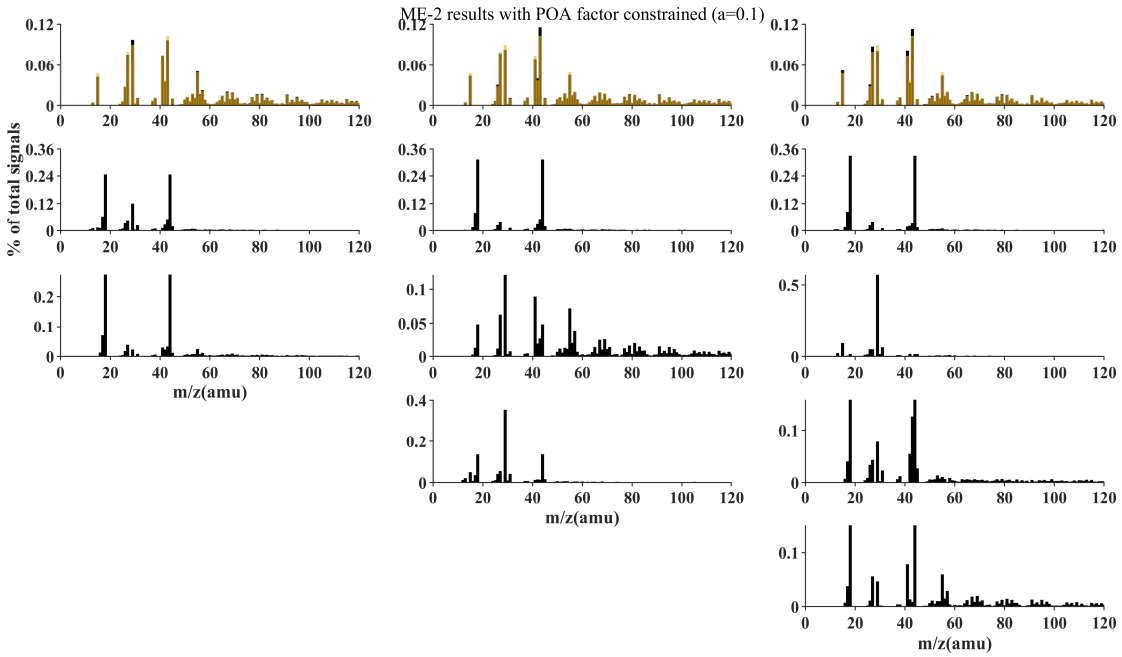

Figure AR5: Mass spectra of 3-5 factor solution from ME-2 analysis (a=0.1) with POA factor constrained for spring. Yellow bar stands for priori POA factor mass spectra from unconstrained 2-factor solution.

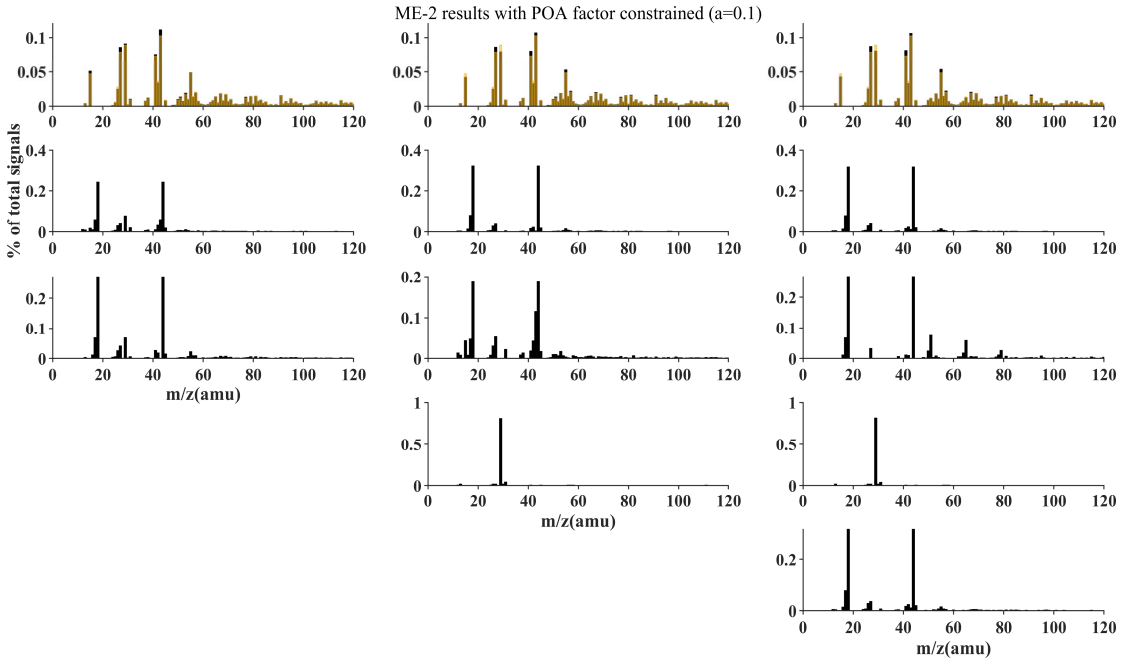

Figure AR6: Mass spectra of 3-5 factor solution from ME-2 analysis (a=0.1) with POA factor constrained for summer. Yellow bar stands for priori POA factor mass spectra from unconstrained 2-factor solution.

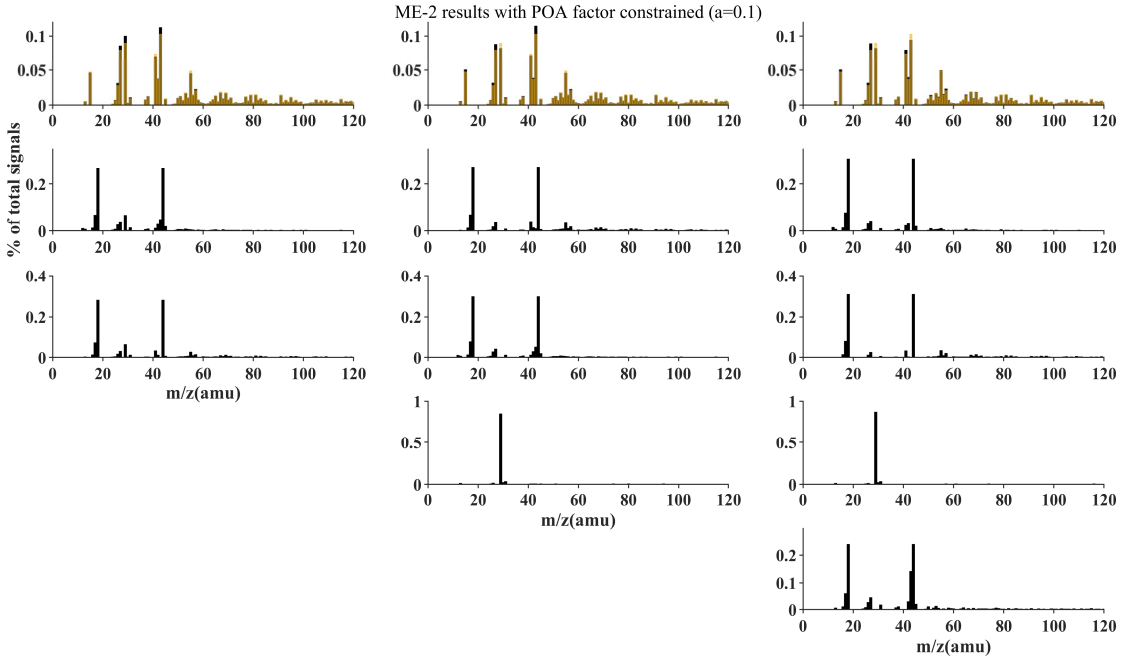

Figure AR7: Mass spectra of 3-5 factor solution from ME-2 analysis (a=0.1) with POA factor constrained for autumn. Yellow bar stands for priori POA factor mass spectra from unconstrained 2-factor solution.

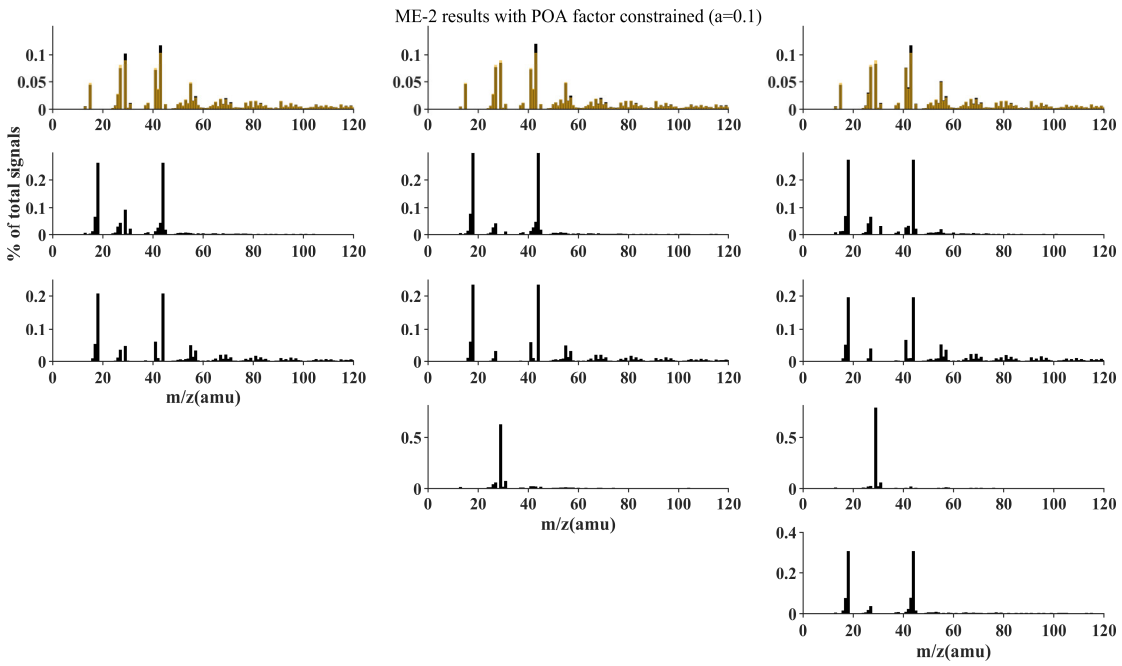

Figure AR8: Mass spectra of 3-5 factor solution from ME-2 analysis (a=0.1) with POA factor constrained for winter. Yellow bar stands for priori POA factor mass spectra from unconstrained 2-factor solution.

We further conducted 3-factor ME-2 analysis with a value ranging from 0.1 to 0.3 (Figure AR9-10). Similar over split features of OOA factors were found in the other seasons with a value of 0.2 or 0.3. As the ME-2 analysis over the entire period gave consistent results of OOA factor splitting, we compared the time-series of OOA factors with secondary inorganic aerosols. It was interesting to note that the MO-OOA had higher correlations with NO_3 (Table AR2), indicating that NO_3 came from aged airmasses, possibly regional background sources. Finally, we compared the mass concentrations of ME-2 OA factors with those of unconstrained factors. The square of correlation coefficients (R^2) between the two methods were 0.97 and 1.00 for POA and OOA, respectively. A portion of 22.3% of unconstrained POA mass further split into OOA in the ME-2 solution. Overall, the ME-2 results did not change the main conclusions of original manuscript, but possible influences were mentioned accordingly.

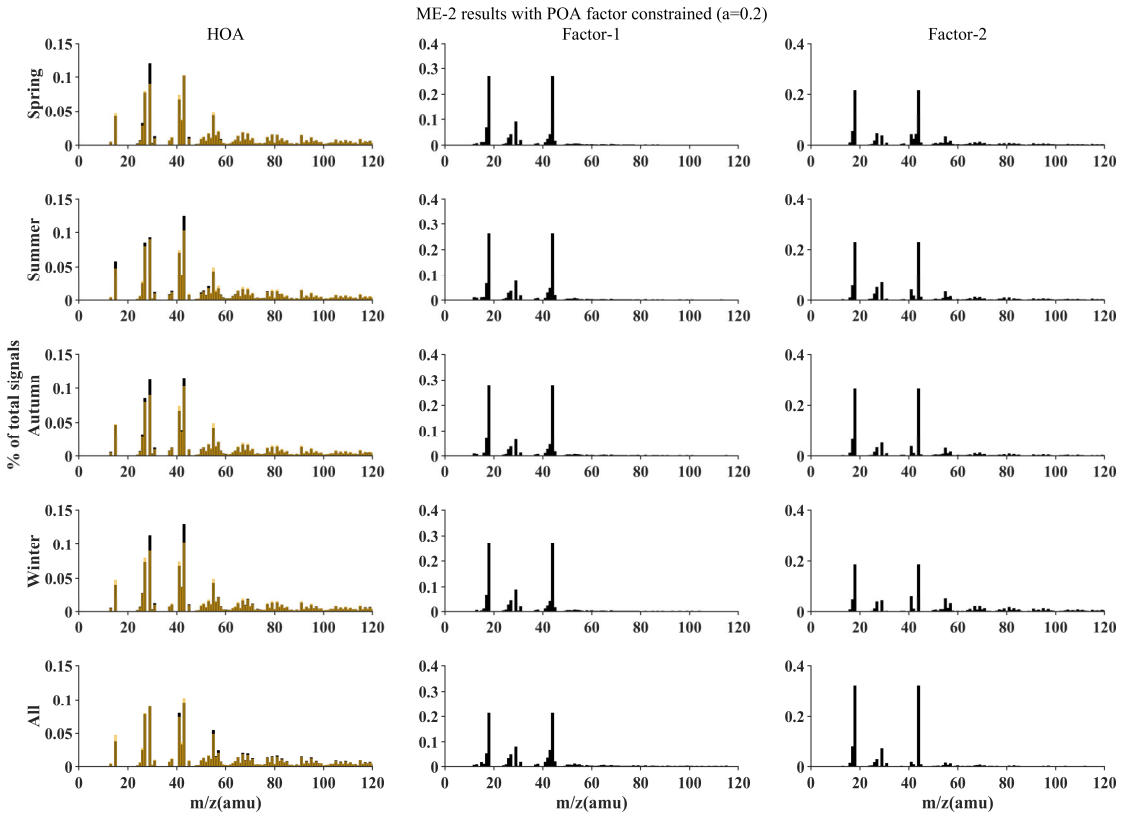

Figure AR9: Mass spectra of 3 factor solution from ME-2 analysis (a=0.2) with POA factor constrained for four seasons and the entire study period.

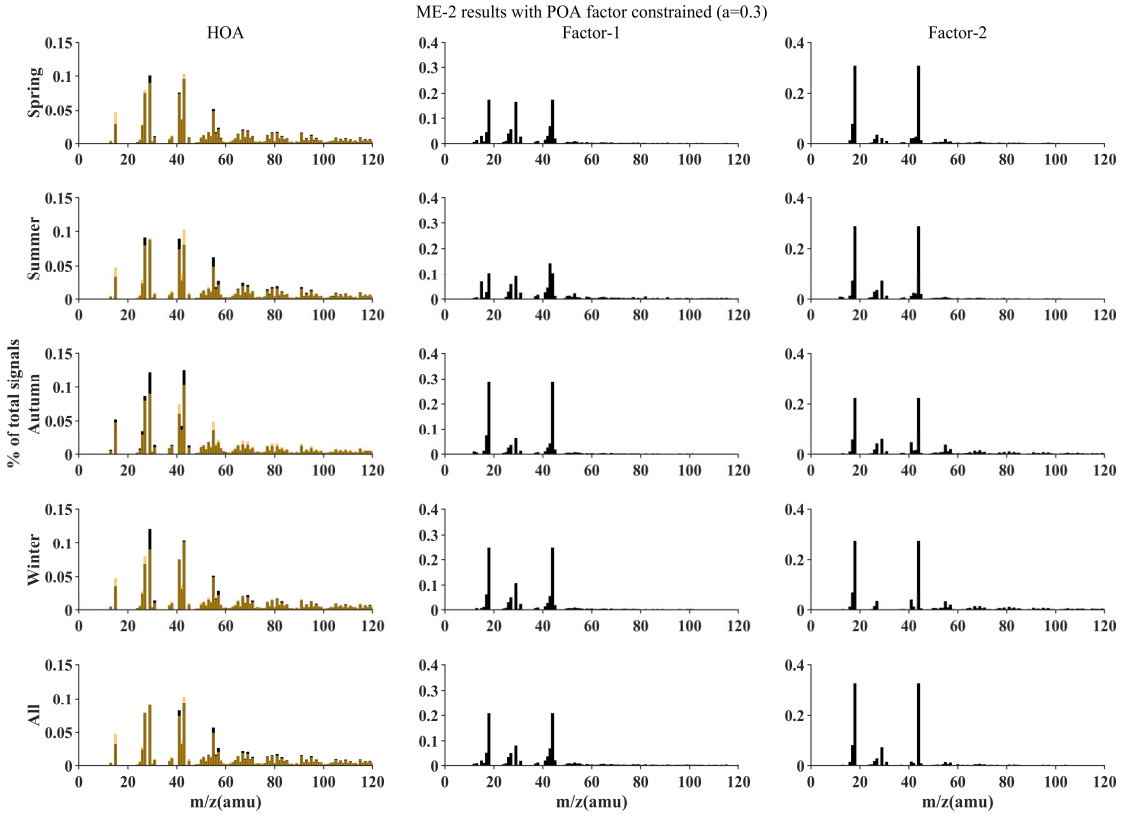

Figure AR10: Mass spectra of 3 factor solution from ME-2 analysis (a=0.3) with POA factor constrained for four seasons and the entire study period.

Table AR2: The correlation coefficients (R^2) between OOA factors from ME-2 solution and secondary inorganic aerosols.

		a=0.1	a=0.2	a=0.3
LO-OOA	SO_4	0.45	0.44	0.44
	NO_3	0.33	0.32	0.32
MO-OOA	SO_4	0.30	0.31	0.32
	NO_3	0.60	0.60	0.60

3. Simultaneous measurements of chemical compositions at Shanghai tower and the ground benefit the comparisons of vertical differences. In line 140-145, the author compared nitrate at SHT with previous studies. The question is that meteorology significantly impacts PM concentrations. The author simply compared the annual average nitrate contribution with surface measurements, without considering the sampling sites, seasons and meteorology. Another question is why higher nitrate aloft owed to lower temperature. Is it possible that other pathways also contribute to nitrate formation?

Response:

Thanks for your suggestion. We summarized NO_3 mass fraction related field observations in Shanghai in Table AR3. We found significantly higher NO_3 mass fractions in spring and winter at SHT than previous surface studies despite sampling sites, instruments, and years. In summer, the fraction at a rural site (Zhao et al., 2020) was found lower but close to this study. According to Cui et al. (2022), the proportion of NO_3 was as high as 26.0% in late autumn of 2018. For a similar period (November) in 2019, the ratio at SHT was 27.2%. We also gathered water-soluble NO_3 from MARGA

observations at SUR, further supporting the higher portion of NO_3 at SHT. We revised the manuscript accordingly.

The SHT and SRF had impacts from similar emission sources to multi-month time scales. The meteorology seems to be the major factor influencing the higher nitrate at SHT. However, other nitrate formation pathways are also possible. Thus, we revised the relevant sentence and focused on presenting observation results there.

Table AR3: The NO_3 mass concentrations and mass fractions in Shanghai.

Description of sampling sites	Instruments (Particle nature)	Seasons (Year)	NO_3 mass concentrations ($\mu g\ m^{-3}$)	NO_3 mass fractions (%)	References
A residential and business area	HR-ToF-AMS (NR-PM_1)	Spring (2016)	3.8±5.7	15.9%	Zhu et al. (2021)
		Summer (2016)	2.9±4.9	10.2%	
		Winter (2017)	7.3±7.0	22.9%	
A residential and business area	HR-ToF-AMS (NR-PM_1)	Spring-early summer (2010)	~4.8	16.3%	Huang et al. (2012)
A commercial and residential district	MARGA (Water-soluble $PM_{2.5}$)	Late autumn (2018)	12.9±12.8	27.2%	He et al. (2020)
Urban	HR-ToF-AMS (NR-PM_1)	Winter (2016)	7.3±6.9	22.1%	Zhu et al. (2018)
Urban	HR-ToF-AMS (NR-PM_1)	Late autumn (2018)	~5.6	26.0%	Cui et al. (2022)
Rural	ACSM (NR-PM_1)	Summer (2015)	~6.5	20.0%	Zhao et al. (2020)
		Autumn (2015)	~9.1	22.0%	

		Winter (2015)	~15.7	26.0%	
		Spring (2016)	~11.2	26.0%	
A central business district	ACSM (NR-PM_1)	Spring (2019)	4.8±4.8	29.9%	This study
		Summer (2019)	3.3±3.2	20.4%	
		Autumn (2019)	3.4±2.9	24.5%	
		Winter (2019)	7.2±7.6	36.8%	
A residential and business area	MARGA (Water-soluble $PM_{2.5}$)	Spring (2019)	7.1	24.5%	This study
		Summer (2019)	4.8	19.6%	
		Autumn (2019)	4.5	18.6%	
		Winter (2019)	12.1	27.7%	

4. The author said throughout the study that SHT is close to the top of PBL but no PBL data was shown. The PBL is dynamically varied during daytime and nighttime, and the PBL height might lower than 600 m under severe haze pollutions.

Response:

Thanks for your suggestion. We obtained PBL height (PBLH) at SHT from the nearest ERA5 gridded reanalysis data (Hersbach et al., 2020) (https://cds.climate.copernicus.eu/cdsapp#!/dataset/reanalysis-era5-single-levels?tab=form, accessed 27 November 2022). The ERA-PBLH is calculated utilizing a bulk Richardson method, which was widely used for both convective and stable boundary layers (Kim, 2022). According to Wang

et al. (2018), the ERA data tend to overestimate PBLH at nighttime, but underestimate PBLH during daytime in Eastern China by comparing with PBLH calculated from radiosonde sounding data. Overall, the reanalysis data can capture the diurnal and seasonal cycle of PBL structure.

As shown in Figure AR11, the autumn found the highest PBLH for its prevailing synoptic of the continental high pressure (characterized as weak winds, strong solar radiation, and dry weather), favorable for the PBL development. PBLH in four seasons presented similar diurnal variations. The PBL started to develop at 06:00-08:00 before reaching a daily top at 13:00-14:00, and then decreased until stabilizing after sunset (18:00-19:00). However, the summertime PBL had the longest development period (06:00-19:00), while the wintertime PBL had the shortest (08:00-18:00). At nighttime, the observatory at SHT generally stood on top of stable BL despite the deviations. Whereas the time PBL top reaching SHT site varied during the day. Nevertheless, the PBL had contact with SHT top even for the lower bound of deviation, indicating inevitable mass exchanges between SHT and SUR during the daytime.

Though we agree with you about the possibility of lower PBLH than 600m under severe haze pollutions, the low occurrence of haze events in Shanghai during the study period might not change the pre-mentioned characteristics of PBLH evolution.

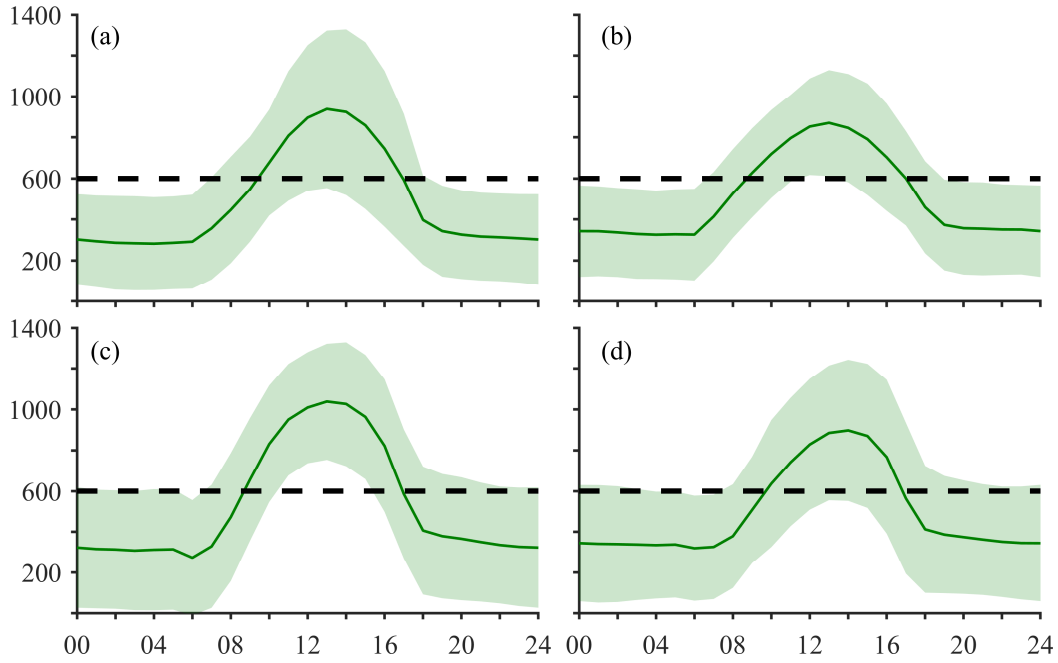

Figure AR11: Diurnal variations of the reanalysis PBL height in spring (a), summer (b), autumn (c), and winter (d) at the grid box where the Shanghai Tower (SHT) site is in. The solid line represents the mean value, and the shaded area stands for the standard deviation. The dash lines represent the altitude (~600 m) of the SHT site.

5. In line 155-165, it is confused that the author described the maximum and minimum temperature and RH in detail solely. In fact, the meteorology was linked to chemical compositions. Discussing the influence and interaction between meteorology and PM is more charming. Why the author showed the daily average values in Table 1?

Response:

We totally agree that the meteorology is closely linked to chemical compositions. We described the maximum and minimum temperature and RH to give a basic concept of the differences between SHT and SUR meteorological environments. More discussion can be found in section 3.3.2. We modified the manuscript to clarify.

We also provided hourly average values in Table AR4, where the statistics had virtually identical mean values to those in Table 1, while larger standard deviations, especially for aerosol species. As we discussed seasonal features of aerosol and meteorology in section 3.1, the deviations of daily average values excluded the effects of intraday fluctuations.

Table AR4: The seasonal and annual averaged concentrations of aerosol species (μg m^{-3}) and meteorological parameters.

		Spring	Summer	Autumn	Winter	Annual
Aerosol Species (μg m^{-3})						
SHT	PM_1	18.5±13.9	16.9±14.3	14.7±11.4	19.7±17.6	17.4±14.6
	$PM_{2.5}$	25.4±17.9	22.8±17.6	22.1±17.0	31.9±28.8	25.7±21.6
	SO_4	3.0±2.4	4.3±2.7	3.1±2.1	3.3±2.7	3.4±2.6
	NO_3	4.8±6.3	3.4±4.3	3.4±4.0	7.2±8.7	4.7±6.4
	NH_4	2.0±1.9	2.0±1.6	1.9±1.4	2.6±2.6	2.1±2.0
	Chl	0.2±0.3	0.2±0.2	0.3±0.2	0.4±0.5	0.3±0.3
	OA	6.0±4.9	6.6±6.3	5.0±3.8	5.8±4.9	5.9±5.2
	POA	1.9±1.9	2.4±2.6	1.4±1.4	1.7±1.6	1.9±2.0
	OOA	4.1±3.2	4.3±3.8	3.6±2.6	4.2±3.5	4.0±3.4
SUR	$PM_{2.5}$	29.1±19.7	24.7±16.0	24.2±18.1	43.6±33.2	30.4±24.1
Meteorological parameters						
SHT	T (°C)	13.3±5.6	22.8±3.5	15.9±4.9	5.9±4.1	14.5±7.6
	RH (%)	61.1±23.6	79.6±11.4	74.9±13.8	72.1±17.3	71.9±18.5
SUR	T (°C)	16.2±5.6	26.5±3.9	19.7±5.5	8.6±4.1	17.7±8.1
	RH (%)	71.0±23.6	82.8±14.8	76.7±18.6	77.5±20.4	77.0±20.1

6. In Sec. 3.2.2, please give the definition of anomaly. Is it calculated by comparing with annual average or history records? Why were they anomaly?

Response:

The anomaly was the monthly deviation from annual average. By calculating the anomaly, we intended to find monthly changes relative to the whole year. The comparison of SHT and SUR PM anomalies allows us to see the consistency of monthly features at two altitudes.

The manuscript was modified to clarify.

7. In line 202-203, the author state that extra aerosol productions contributed to higher $PM_{2.5}$ concentrations at SHT than surface. Please elaborate the conclusion.

Response:

Given that SHT was farther from the direct emission sources than SUR, the $PM_{2.5}$ at SHT tended to have lower concentration than SUR as in the other months despite vertical mixing during the daytime. Thus, the higher $PM_{2.5}$ at SHT in August indicated extra aerosol productions at mid-upper PBL.

8. In line 205-210, the author said that exchange between SHT and surface only exits in daytime. If nocturnal PBL is higher than SHT, nighttime exchange can also occur. Nighttime $PM_{2.5}$ at SHT was not independent from the ground level.

Response:

As discussed in the response of question 4, it's true that the exchange between SHT and surface only exits in daytime, at least in the view of ERA5-PBLH. However, we acknowledge that the PBLH is crucial for the vertical structure analysis, and direct observations of PBLH are in need to give precise view of concurrent boundary layer processes. We mentioned this factor in the conclusion part.

9. In Sec. 3.2.4 and figure 4, the author can also plot and discuss mass fractions of NR-PM_1 during daytime and nighttime separately.

Response:

Thanks for your suggestion, and figure 4 was revised and discussed accordingly:

The daytime and nighttime mass fractions were shown in Figure AR12. As results of vertical mixing, the larger portions of primary species (POA and Chl) during daytime were notable, especially for summer and autumn. The changes of OOA, NO_3, and NH_4 were slight, with increase of OOA and NH_4, but decrease of NO_3 from nighttime to daytime. Accordingly, SO_4 saw lower fraction in NR-PM_1 during the daytime. More diurnal features of NR-PM_1 can be found in section 3.3.4.

But as you mentioned in question 3, "simultaneous measurements of chemical compositions at Shanghai tower and the ground benefit the comparisons of vertical differences". The lack of surface measurements of chemical compositions prevented us from digging more into the vertical differences between SHT and SUR.

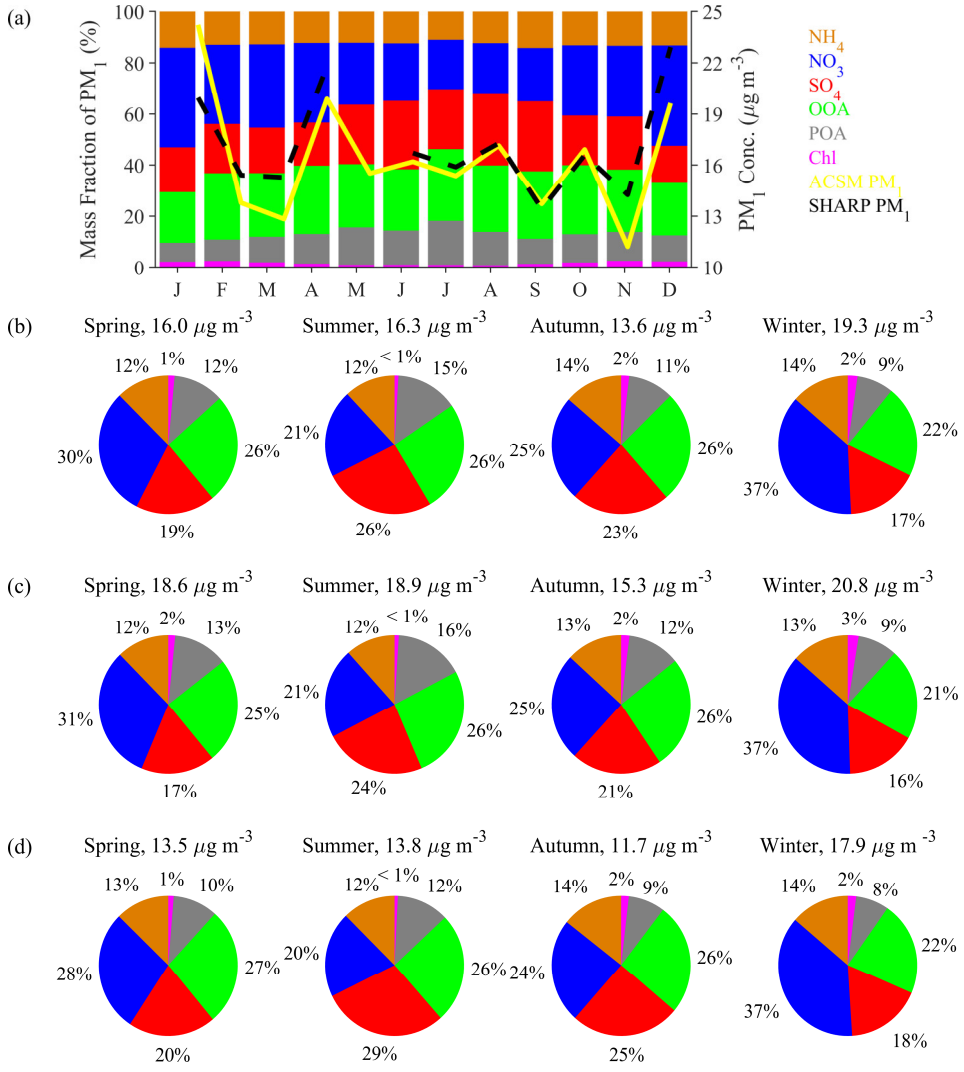

Figure AR12: The monthly averaged (a) and seasonal averaged (b-d) mass fractions (%) of NR-PM_1 at SHT. The mass fractions (%) are calculated based on all (b), daytime (c), and nighttime (d) data. The monthly averaged mass concentrations (μg m^{-3}) of NR-PM_1 are also shown. The solid and dashed line represent SHARP PM_1 and NR-PM_1, respectively.

10. In figure 6, NO_2 at SHT increased by 21.8-61.4% from 08:00 to 12:00, while they were reduced at ground level during this time. Thus, vertical mixing could be the explanation rather than vehicles. In fact, the peak at morning at surface was attributed to traffic during morning rush hour.

Response:

Thank you for the note. The corresponding sentences were corrected.

11. In line 62, "vatical distribution" might be a typo.

Response:

Thank you. It was revised to 'vertical distribution'.

12. Please uniform the subscripts of sulfate, nitrate and ammonium throughout the study.

Response:

Thank you. We rechecked the relevant subscripts.

References:

Canonaco, F., Crippa, M., Slowik, J. G., Baltensperger, U., and Prevot, A. S. H.: SoFi, an IGOR-based interface for the efficient use of the generalized multilinear engine (ME-2) for the source

apportionment: ME-2 application to aerosol mass spectrometer data, Atmospheric Measurement Techniques, 6, 3649-3661, 10.5194/amt-6-3649-2013, 2013.

Cui, S. J., Huang, D. D., Wu, Y. Z., Wang, J. F., Shen, F. Z., Xian, J. K., Zhang, Y. J., Wang, H. L., Huang, C., Liao, H., and Ge, X. L.: Chemical properties, sources and size-resolved hygroscopicity of submicron black-carbon-containing aerosols in urban Shanghai, Atmospheric Chemistry and Physics, 22, 8073-8096, 10.5194/acp-22-8073-2022, 2022.

He, X., Wang, Q. Q., Huang, X. H. H., Huang, D. D., Zhou, M., Qiao, L. P., Zhu, S. H., Ma, Y. G., Wang, H. L., Li, L., Huang, C., Xu, W., Worsnop, D. R., Goldstein, A. H., and Yu, J. Z.: Hourly measurements of organic molecular markers in urban Shanghai, China: Observation of enhanced formation of secondary organic aerosol during particulate matter episodic periods, Atmospheric Environment, 240, 10.1016/j.atmosenv.2020.117807, 2020.

Hersbach, H., Bell, B., Berrisford, P., Hirahara, S., Horanyi, A., Munoz-Sabater, J., Nicolas, J., Peubey, C., Radu, R., Schepers, D., Simmons, A., Soci, C., Abdalla, S., Abellan, X., Balsamo, G., Bechtold, P., Biavati, G., Bidlot, J., Bonavita, M., De Chiara, G., Dahlgren, P., Dee, D., Diamantakis, M., Dragani, R., Flemming, J., Forbes, R., Fuentes, M., Geer, A., Haimberger, L., Healy, S., Hogan, R. J., Holm, E., Janiskova, M., Keeley, S., Laloyaux, P., Lopez, P., Lupu, C., Radnoti, G., de Rosnay, P., Rozum, I., Vamborg, F., Villaume, S., and Thepaut, J. N.: The ERA5 global reanalysis, Quarterly Journal of the Royal Meteorological Society, 146, 1999-2049, 10.1002/qj.3803, 2020.

Huang, X. F., He, L. Y., Xue, L., Sun, T. L., Zeng, L. W., Gong, Z. H., Hu, M., and Zhu, T.: Highly time-resolved chemical characterization of atmospheric fine particles during 2010 Shanghai World Expo, Atmospheric Chemistry and Physics, 12, 4897-4907, 10.5194/acp-12-4897-2012, 2012.

Kim, K.-Y.: Diurnal and seasonal variation of planetary boundary layer height over East Asia and its climatic change as seen in the ERA-5 reanalysis data, SN Applied Sciences, 4, 39, 10.1007/s42452-021-04918-5, 2022.

Middlebrook, A. M., Bahreini, R., Jimenez, J. L., and Canagaratna, M. R.: Evaluation of composition-dependent collection efficiencies for the Aerodyne aerosol mass spectrometer using field data, Aerosol Sci. Technol., 46, 258-271, 10.1080/02786826.2011.620041, 2012.

Wang, Y. J., Xu, X. D., Zhao, Y., and Wang, M. Z.: Variation characteristics of the planetary boundary layer height and its relationship with PM2.5 concentration over China, Journal of Tropical Meteorology, 24, 385-394, 10.16555/j.1006-8775.2018.03.011, 2018.

Zhao, Q. B., Huo, J. T., Yang, X., Fu, Q. Y., Duan, Y. S., Liu, Y. X., Lin, Y. F., and Zhang, Q.: Chemical characterization and source identification of submicron aerosols from a year-long real-time observation at a rural site of Shanghai using an Aerosol Chemical Speciation Monitor, Atmospheric Research, 246, 10.1016/j.atmosres.2020.105154, 2020.

Zhu, W., Zhou, M., Cheng, Z., Yan, N., Huang, C., Qiao, L., Wang, H., Liu, Y., Lou, S., and Guo, S.: Seasonal variation of aerosol compositions in Shanghai, China: Insights from particle aerosol mass spectrometer observations, Science of The Total Environment, 771, 144948, 10.1016/j.scitotenv.2021.144948, 2021.

Zhu, W. F., Xie, J. K., Cheng, Z., Lou, S. R., Luo, L. N., Hu, W. W., Zheng, J., Yan, N. Q., and Brooks, B.: Influence of chemical size distribution on optical properties for ambient submicron particles during severe haze events, Atmospheric Environment, 191, 162-171, 10.1016/j.atmosenv.2018.08.003, 2018.